Orphan G Protein–Coupled Receptor GPR116 Regulates Pulmonary Surfactant Pool Size

James P. Bridges[1], Marie-Gabrielle Ludwig[2], Matthias Mueller[2], Bernd Kinzel[2], Atsuyasu Sato[1], Yan Xu[1], Jeffrey A. Whitsett[1], and Machiko Ikegami[1]

[1]Perinatal Institute, Division of Pulmonary Biology, Cincinnati Children's Hospital Medical Center, Cincinnati, Ohio; and [2]Novartis Institutes for Biomedical Research, Basel, Switzerland

Pulmonary surfactant levels within the alveoli are tightly regulated to maintain lung volumes and promote efficient gas exchange across the air/blood barrier. Quantitative and qualitative abnormalities in surfactant are associated with severe lung diseases in children and adults. Although the cellular and molecular mechanisms that control surfactant metabolism have been studied intensively, the critical molecular pathways that sense and regulate endogenous surfactant levels within the alveolus have not been identified and constitute a fundamental knowledge gap in the field. In this study, we demonstrate that expression of an orphan G protein–coupled receptor, GPR116, in the murine lung is developmentally regulated, reaching maximal levels 1 day after birth, and is highly expressed on the apical surface of alveolar type I and type II epithelial cells. To define the physiological role of GPR116 *in vivo*, mice with a targeted mutation of the *Gpr116* locus, *Gpr116*$^{\Delta exon17}$, were generated. *Gpr116*$^{\Delta exon17}$ mice developed a profound accumulation of alveolar surfactant phospholipids at 4 weeks of age (12-fold) that was further increased at 20 weeks of age (30-fold). Surfactant accumulation in *Gpr116*$^{\Delta exon17}$ mice was associated with increased saturated phosphatidylcholine synthesis at 4 weeks and the presence of enlarged, lipid-laden macrophages, neutrophilia, and alveolar destruction at 20 weeks. mRNA microarray analyses indicated that P2RY2, a purinergic receptor known to mediate surfactant secretion, was induced in *Gpr116*$^{\Delta exon17}$ type II cells. Collectively, these data support the concept that GPR116 functions as a molecular sensor of alveolar surfactant lipid pool sizes by regulating surfactant secretion.

Keywords: pulmonary surfactant; G protein–coupled receptors; GPR116; surfactant metabolism; alveolar epithelium

CLINICAL RELEVANCE

The molecular pathways that sense and regulate surfactant levels in the alveolar saccules are incompletely understood. In this work we provide evidence that the G protein–coupled receptor GPR116 is a master regulator of surfactant homeostasis. The long-term goal of this work is to identify potential therapeutic targets, including GPR116, for modulating endogenous surfactant levels in the treatment of lung disease.

Pulmonary surfactant is synthesized by alveolar type II cells and is primarily composed of phospholipids, which constitute 80% of the total mass. The remaining components include neutral lipids, the lipid-associated surfactant proteins SFTPB and SFTPC, and the hydrophilic surfactant proteins SFTPA and SFTPD (1, 2). Saturated phosphatidylcholine (SatPC) is uniquely enriched in surfactant and, in concert with SFTPB and SFTPC, is fundamentally required to reduce surface tension at the air/liquid interface within the alveolus (3, 4). After synthesis, the lipid and lipid-associated proteins SFTPB and SFTPC are routed to and stored in membrane-enclosed secretory organelles called lamellar bodies. Through constitutive pathways or upon stimulation by secretagogues (including purines [5, 6], β-agonists [7–9], and adenosine [10, 11]) or mechanical stretch (12), lamellar bodies fuse with the plasma membrane and are exocytosed from type II cells into the alveolar space.

The quantity of surfactant in the mammalian lung, referred to as surfactant pool size, increases dramatically during late gestation to facilitate the transition to air breathing at birth. In the fetal lung, the majority of surfactant is stored within type II cells, with minimal amounts of secreted surfactant in the airspace. During the fetal-to-neonatal transition, stored surfactant is rapidly secreted into the alveoli; tissue and alveolar pool levels subsequently decline within 2 to 5 days due to decreased secretory rates and increased catabolic rates (13–15). Alveolar surfactant pool sizes are tightly regulated and maintained at a steady-state level in the adult lung through a net balance of synthesis, secretion, and recycling by alveolar type II cells and by catabolism by alveolar macrophages and type II cells (16). Alterations in surfactant pool size or composition significantly affect lung function and have been associated with severe lung diseases in children and adults, including respiratory distress syndrome, acute lung injury, chronic lung disease, and pulmonary alveolar proteinosis. The ability to pharmacologically manipulate pathways that modulate endogenous surfactant pool sizes, both positively and negatively, may provide therapeutic benefit for diseases associated with dysregulation of the surfactant system.

Secretion of surfactant-containing lamellar bodies from type II cells occurs by two pathways: constitutive and regulated secretion. Three G protein–coupled receptor (GPCR)-mediated pathways have been implicated in controlling regulated secretion from isolated type II cells: the P2RY2 purinoreceptor pathway, the β_2 adrenergic receptor (β_2AR) pathway, and the adenosine A_{2B} pathway (5–10). Activation of these G protein–coupled pathways by their cognate agonists results in increased cytosolic levels of the second messengers Ca^{2+} and/or cAMP, culminating in the activation of one or more of three downstream protein kinases, protein kinase (PK)A, PKC, and Ca^{2+}/calmodulin-dependent protein kinase, that lead to surfactant release (17–20). Likewise, compounds that bypass the receptors to activate PKA or PKC

(*Received in original form October 31, 2012 and in final form March 13, 2013*)

This work was supported by divisional start-up funds, a Perinatal Institute Pilot and Feasibility grant, and a Trustee grant from Cincinnati Children's Hospital Medical Center (J.P.B.) and by National Institutes of Health grants HL110964 (J.A.W.) and HL105433 (Y.X.).

Correspondence and requests for reprints should be addressed to James P. Bridges, Ph.D., Cincinnati Children's Hospital Medical Center, Perinatal Institute, Division of Pulmonary Biology, 3333 Burnet Avenue, ML7029, Cincinnati, OH 45229. E-mail: James.Bridges@cchmc.org

This article has an online supplement, which is accessible from this issue's table of contents at www.atsjournals.org.

Am J Respir Cell Mol Biol Vol 49, Iss. 3, pp 348–357, Sep 2013
Copyright © 2013 by the American Thoracic Society
Originally Published in Press as DOI: 10.1165/rcmb.2012-0439OC on April 5, 2013
Internet address: www.atsjournals.org

directly or that increase cytosolic Ca^{2+} levels are sufficient to stimulate surfactant secretion *in vitro* (7, 9, 21). Mechanical stretch of isolated type II cells *in vitro* or by hyperventilation *ex vivo* is the most physiologically relevant stimulus identified to date and induces surfactant secretion via ATP- and Ca^{2+}–dependent pathways (12, 22). Although many exogenous extracellular and intracellular mediators are capable of stimulating surfactant secretion *in vitro*, the endogenous, physiologically dominant *in vivo* agonists and receptors that control surfactant pool sizes have not been established.

In the present study, we report that an orphan member of the adhesion GPCR family, GPR116, is highly expressed on alveolar epithelial cells and that mice with a genetic loss of GPR116 function, *Gpr116*$^{\Delta exon17}$, have a marked accumulation of pulmonary surfactant that is progressive in nature. We further demonstrate that incorporation of surfactant precursors into SatPC was increased in *Gpr116*$^{\Delta exon17}$ mice and that surfactant accumulation was associated with increased expression of P2RY2, a GPCR known to mediate surfactant secretion, in alveolar type II cells. Collectively, these data demonstrate that GPR116 is a major regulator of surfactant homeostasis.

MATERIALS AND METHODS

Generation of *Gpr116*$^{\Delta exon17}$ Animals and GPR116 Antisera

Details regarding the generation of *Gpr116*$^{\Delta exon17}$ animals and GPR116 antisera are listed in the online data supplement and Figure E1 in the online supplement.

Saturated Phosphatidylcholine Measurements

Bronchoalveolar lavage fluid (BALF) was collected by intratracheal intubation followed by serial lavaging with 0.9% saline (5 × 1 ml total, pooled and placed on ice). BAL cells were isolated from the lavage via centrifugation at 900 × *g* for 10 minutes at 4°C. After lavage, lungs were homogenized in 0.9% saline. Lipids were extracted from the lavage and postlavaged lung homogenate by the Bligh and Dyer method (23). SatPC was isolated using the osmium tetroxide–based method of Mason and colleagues (24) and quantitated by phosphorous measurement. SatPC levels in BALF reported in this manuscript represent the total BALF, including the BAL cell pellet, due to our inability to reliably and accurately separate the BAL cells from the abnormally aggregated surfactant in the BALF of *Gpr116*$^{\Delta exon17}$ animals; SatPC levels reported in the lung homogenate are from postlavaged lung homogenate.

Phospholipid Composition and SatPC Synthesis Measurements

Phospholipid composition was performed on chloroform-methanol extracts of BALF by two-dimensional thin-layer chromatography as previously described (25). SatPC synthesis was determined *in vivo* as previously described using [3H]-palmitic acid and [methyl-3H]-choline chloride (25). Briefly, 0.5 μCi [3H]-palmitic acid or [3H]-choline chloride/g body weight was injected intraperitoneally into 4-week-old wild-type (WT) and *Gpr116*$^{\Delta exon17}$ mice. Eight hours after injection, BALF and lavaged lung tissue were harvested, SatPC was isolated, and radioactivity was determined in the SatPC fraction. The 8-hour time point was chosen for this analysis because we have previously shown this time point to best reflect the net incorporation of precursor into SatPC and secretion of labeled SatPC into the alveoli with minimal recycling and catabolism of labeled SatPC by type II cells and alveolar macrophages (26).

RNA Isolation and Real-Time PCR Analysis

Total RNA was purified from adult murine organs, whole lung homogenates, or isolated type II cell preparations with the RNeasy Mini Kit (Qiagen, Valencia, CA) and reverse transcribed into cDNA with the iScript kit (BioRad, Hercules, CA). Real-time qPCR was performed on a 7300 real-time PCR system (Applied Biosystems, Foster City, CA) with TaqMan gene expression assays (Table E1) and normalized to endogenous *ActinB*.

Histology, Immunohistochemistry, and Western Blot Analysis

Details are provided in the online supplement.

Transmission Electron Microscopy

Lungs from 20-week-old animals were fixed, processed, and analyzed as previously described (27).

Isolation, Culture, and SatPC Analysis of Adult Type II Cells

Details are provided in the online supplement.

Isolation of Lamellar Bodies

Details are provided in the online supplement.

Statistical Analysis

All data are presented as means ± SEM, with $P \leq 0.05$ considered significant. Multiple group comparisons were made by one-way ANOVA with a Tukey *post hoc* analysis. Two-way comparisons were performed by two-tailed, unpaired Student's *t* test. All analyses were performed using GraphPad Prism software version 5.0.

RESULTS

GPR116 Expression in the Murine Lung

We first sought to define the expression pattern of murine *Gpr116* by analyzing several tissues via real-time qPCR. *Gpr116* mRNA was detectable in multiple organs of the adult mouse and was highly expressed in the lung (Figure 1A). These data are consistent with the expression profile of GPR116 in the adult rat (28). To define the developmental expression pattern of GPR116 in the lung, an ontogenic study of *Gpr116* mRNA was performed using lung tissue from E11.5 embryos through 8-week-old adult mice. *Gpr116* mRNA was developmentally regulated in the murine lung, reaching peak expression at postnatal Day 1 with maintenance of high expression levels throughout adulthood (Figure 1B). The sharp increase in *Gpr116* expression in late gestation is temporally consistent with maturation of the surfactant system in alveolar type II cells. To assess the relative degree to which *Gpr116* is expressed in distal epithelial cells, *Gpr116* mRNA expression in primary adult type II cells was quantitated and compared with *Sftpc*, a gene that is highly expressed in type II cells. *Gpr116* mRNA expression is comparable with *Actin* and 7.9-fold lower than *Sftpc* (Figure 1C).

To determine which cell types within the lung express GPR116 protein, immunohistochemistry was performed on adult lung sections with polyclonal antisera directed against the C-terminus of GPR116. In the distal airspaces, GPR116 protein is expressed on the apical surface of type I and type II epithelial cells (Figure 1D, *inset*), consistent with data reported in adult rat lung (28). In the proximal airways, GPR116 is present on ciliated cells (Figure 1D, *arrowheads*) but is not detected on other epithelial cells, including club cells (Clara cells) and neuroendocrine cells. Although *Gpr116* mRNA is expressed in transformed endothelial cell lines (29) and isolated mouse lung endothelial cells (30), GPR116 protein is undetectable in pulmonary endothelial cells analyzed by flow cytometry (Figure E2), and *Gpr116* mRNA and protein are not expressed in alveolar macrophages (data not shown).

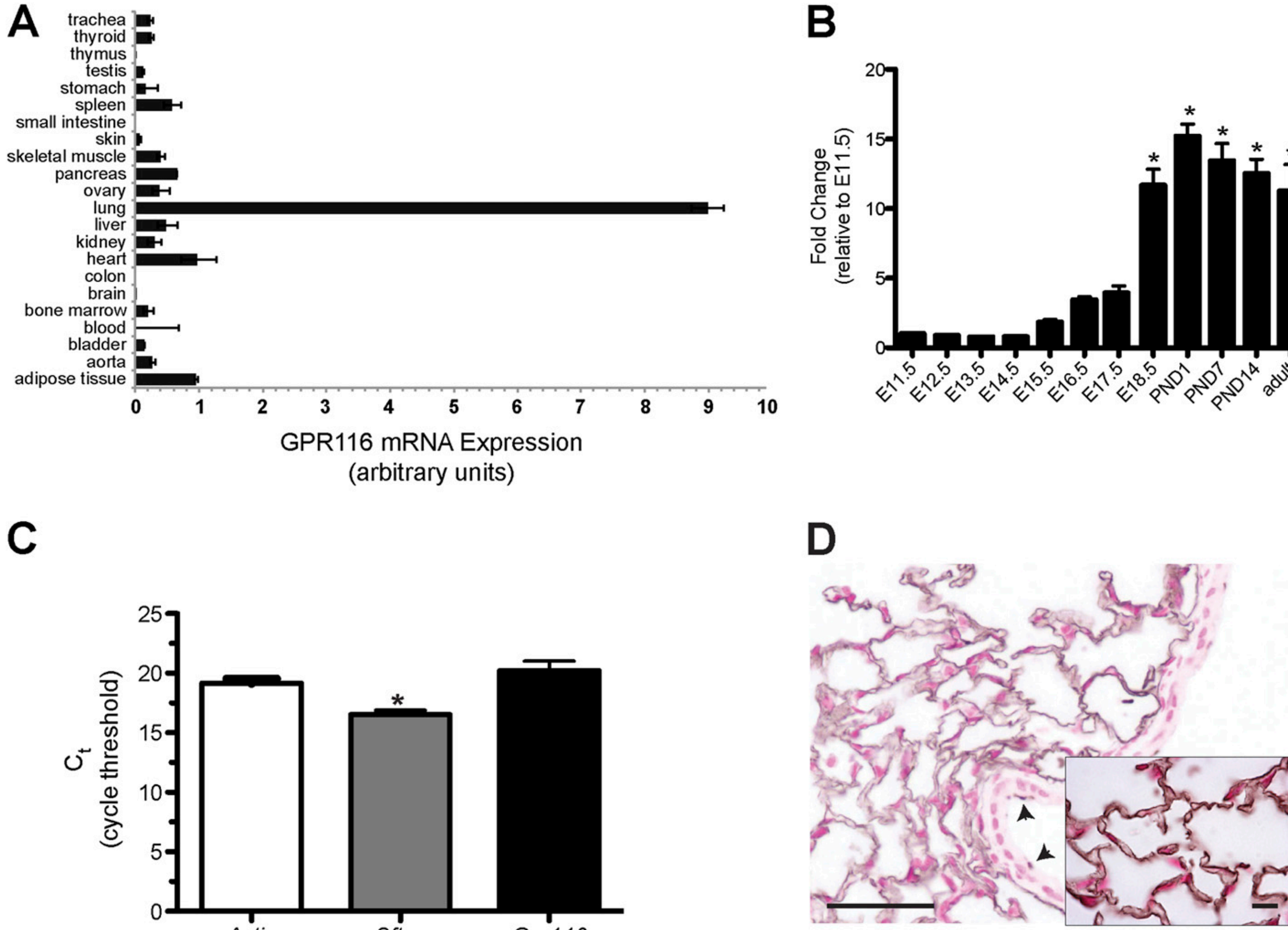

Figure 1. GPR116 expression is enriched in type I and type II alveolar epithelial cells. (*A*) GPR116 mRNA expression in adult mouse tissues measured by qPCR analysis. Note the high expression in lung tissue ($n = 4$ samples per tissue). (*B*) Ontogeny of GPR116 mRNA expression in developing mouse lung. Note the dramatic increase just before birth at E18.5 ($n = 3$ lungs per gestational age). *$P < 0.05$ versus E11.5. (*C*) Quantitation of *Gpr116*, *Sftpc*, and *Actin* mRNA expression by qPCR analysis in type II cells isolated from wild-type (WT) mice ($n = 3$ individual isolations). *$P < 0.05$ versus *Actin*. (*D*) GPR116 immunostaining of adult WT lung with an antibody directed against C-terminus. Note staining of cilia on proximal airway cells (*arrowheads*) and apical staining pattern on type I and type II epithelial cells (*inset*). *Scale bar* = 50 μm in the *large panel* and 10 μm in *inset*.

Generation of GPR116 Loss-of-Function Allele

To define the role of GPR116 *in vivo*, we generated mice with a conditional allele of *Gpr116* by inserting loxP sites into the intronic sequences flanking exon17, which encodes all seven transmembrane domains of GPR116 (Figure E1A). Successful generation of the *Gpr116* floxed allele was confirmed by Southern blot and PCR analyses (Figures E1B and E1C). To ablate GPR116 function in all tissues, *Gpr116*$^{f/f}$ mice were crossed to CMV-Cre transgenic mice and backcrossed to BALB/c mice to remove the CMV-Cre transgene. Homozygous germline GPR116 loss-of-function mice, resultant from heterozygous parents backcrossed to BALB/c mice for more than 12 generations, were used exclusively in this study and are herein referred to as *Gpr116*$^{\Delta exon17}$ mice.

Homozygous *Gpr116*$^{\Delta exon17}$ mice were born at normal Mendelian ratios and were viable, indicating that GPR116 is dispensable for normal embryonic development. Perinatal development of *Gpr116*$^{\Delta exon17}$ mice was normal, as demonstrated by body weights that were comparable to WT control mice from E16.5 through 12 weeks of age (data not shown). To confirm the loss of *Gpr116* mRNA in *Gpr116*$^{\Delta exon17}$ mice, qPCR analyses was performed on *Gpr116*$^{\Delta exon17}$ lung tissue using a TaqMangene expression assay targeting the exon16/17 boundary of *Gpr116*. *Gpr116* mRNA was undetectable in *Gpr116*$^{\Delta exon17}$ lung tissue with this assay, indicating complete ablation of exon17 (Figure E3A). However, using a distinct gene expression assay specific for the exon4/5 boundary, we were able to detect *Gpr116* mRNA in *Gpr116*$^{\Delta exon17}$ lung tissue (Figure E3B). These data demonstrated that the *Gpr116*$^{\Delta exon17}$ allele generated mRNA that was devoid of exon17. Because exon18 is in frame with exon16, it was possible that the *Gpr116*$^{\Delta exon17}$ mRNA was capable of generating a protein that contained exon sequences downstream of exon17. To test this possibility, *Gpr116*$^{\Delta exon17}$ lung sections were stained with GPR116 polyclonal antisera. GPR116 immunoreactivity was indeed observed in distal alveolar epithelial cells of *Gpr116*$^{\Delta exon17}$ mice, albeit at reduced levels and in a discontinuous staining pattern compared with WT control mice (Figure E3C). Consistent with these data, transient expression of human GPR116 cDNA in which exon 17 was deleted in HEK293 cells resulted in diffuse, cytoplasmic staining compared with the uniform localization of the WT protein to the plasma membrane (Figure E3D). Expression and mislocalization of GPR116$^{\Delta exon17}$ protein did not invoke the unfolded protein response, as demonstrated by similar levels of *Hsp15* (*BiP*), *Ddit3* (*CHOP*), and spliced *Xbp-1* in isolated WT and *Gpr116*$^{\Delta exon17}$ type II cells (Figure E3E). Collectively, these results demonstrate that targeting of exon17 in *Gpr116*$^{\Delta exon17}$ mice was successful and that the *Gpr116*$^{\Delta exon17}$ allele generates a protein product devoid of the transmembrane domains encoded by exon17 that is low in abundance, fails to traffic to the plasma membrane, and does not elicit an unfolded protein response in type II cells.

Progressive Pulmonary Surfactant Accumulation in *Gpr116*$^{\Delta exon17}$ Mice

Young *Gpr116*$^{\Delta exon17}$ mice appeared healthy and were phenotypically indistinguishable from heterozygous and WT littermate control mice. However, the majority of *Gpr116*$^{\Delta exon17}$ mice exhibited signs of severe respiratory distress, including profound tachypnea and chest retractions, between 20 and 32 weeks of age. Consistent with these observations, BALF from 20-week-old animals in respiratory distress was extremely turbid and viscous compared with BALF from WT control mice, indicative of increased lipid and/or protein content (Figure E4A).

To determine if surfactant phospholipids were increased in *Gpr116*$^{\Delta exon17}$ mice, SatPC levels in BALF and lung homogenate were quantified at three ages: E18.5, 4 weeks, and 20 weeks. SatPC levels in lung homogenate were comparable in *Gpr116*$^{\Delta exon17}$ and WT control mice at E18.5. However, alveolar and tissue SatPC levels were significantly increased in *Gpr116*$^{\Delta exon17}$ mice at 4 weeks of age (BALF increase, 13.9-fold; lavaged lung homogenate increase, 3.7-fold) and further increased at 20 weeks of age (BALF increase, 33.3-fold; lavaged lung homogenate incease, 29.8-fold) (Figure 2A). Furthermore, the amount of SatPC in the alveoli compared with the amount of SatPC in the total lung, referred to as the SatPC alveolar–tissue index, was increased 2.2-fold in *Gpr116*$^{\Delta exon17}$ mice over WT control mice at 4 weeks of age (Figure 2B). Next, we quantitated SatPC levels in media and the lysates of primary WT and *Gpr116*$^{\Delta exon17}$ type II cells isolated from 4-week-old animals and cultured for 7 days. SatPC levels in WT and *Gpr116*$^{\Delta exon17}$ type II cells were comparable after 7 days of culture, whereas SatPC levels were increased 1.9-fold in the media of *Gpr116*$^{\Delta exon17}$ cells (Figure 2C). Mice heterozygous for the *Gpr116*$^{\Delta exon17}$ allele had SatPC levels comparable to WT mice at 6 months of age (data not shown).

SatPC synthesis rates were evaluated in *Gpr116*$^{\Delta exon17}$ mice by independently measuring the incorporation of two radiolabeled phospholipid precursors, palmitic acid or choline, into SatPC *in vivo*. Incorporation of palmitic acid and choline into SatPC was increased over 2-fold in BALF and lung homogenate of *Gpr116*$^{\Delta exon17}$ mice at 4 weeks of age (Figures 3A and 3B). To determine if SatPC was uniquely enriched in *Gpr116*$^{\Delta exon17}$ mice or if all surfactant phospholipid species were increased proportionately with SatPC, the composition of surfactant phospholipid species in the lavage fluid was quantified by two-dimensional thin-layer chromatography. All of the major phospholipid species examined, including phosphatidylcholine, phosphatidylglycerol, phosphatidylethanolamine, phosphatidylinositol, sphingomyelin, phosphatidylserine, and lysobisphosphatidic acid, were present at comparable levels in the lavage of *Gpr116*$^{\Delta exon17}$ and WT mice (Figure 3C). Taken together, these data demonstrate that *Gpr116*$^{\Delta exon17}$ mice exhibited profound increases of alveolar and tissue surfactant phospholipid pool sizes that initiated in the postnatal period and progressed throughout adulthood. The accumulation of SatPC was associated with an increased SatPC alveolar–tissue index and synthesis *in vivo* and with SatPC accumulation in the media of isolated *Gpr116*$^{\Delta exon17}$ type II cells *in vitro*. Furthermore, all of the major surfactant phospholipid species examined increased proportionately with SatPC in *Gpr116*$^{\Delta exon17}$ animals at 4 weeks of age.

Surfactant Protein Levels in *Gpr116*$^{\Delta exon17}$ Mice

To determine if surfactant protein production and alveolar levels were influenced by GPR116, surfactant protein levels were quantitated from the lavage and lung homogenate of *Gpr116*$^{\Delta exon17}$ and WT animals. Due to the large increase of alveolar SatPC pools in *Gpr116*$^{\Delta exon17}$ mice, inputs for the BALF samples used

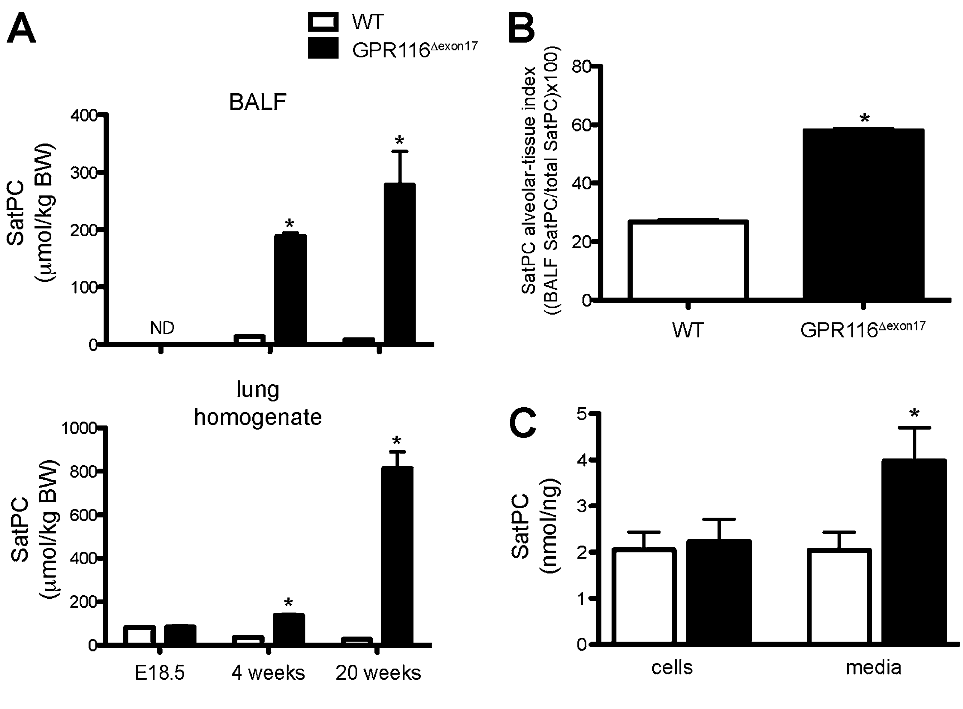

Figure 2. Progressive pulmonary surfactant accumulation in *Gpr116*$^{\Delta exon17}$ mice. (*A*) Saturated phosphatidylcholine (SatPC) levels in bronchoalveolar lavage fluid (BALF) and lung homogenate after BAL isolated by lipid extraction and osmium tetroxide chromatography followed by phosphorous analysis. SatPC levels were similar at E18.5 and significantly increased in 4- and 20-week-old *Gpr116*$^{\Delta exon17}$ mice (n = 4–6 lungs per group). BW = body weight; ND = not determined due to inability of lavaging E18.5 animals. (*B*) SatPC alveolar–tissue index, calculated from 4-week data in panel *A* [(SatPC in BALF)/(SatPC in BALF + SatPC in lung tissue)], was increased 2.2-fold in *Gpr116*$^{\Delta exon17}$ mice. (*C*) Cumulative SatPC levels in cell lysates and media from isolated type II cells cultured for 7 days. SatPC in the media of *Gpr116*$^{\Delta exon17}$ type II cells was increased 2.0-fold compared with WT. Data are pooled from four individual isolations (n = 2 mice/genotype/isolation). *$P < 0.05$ versus WT.

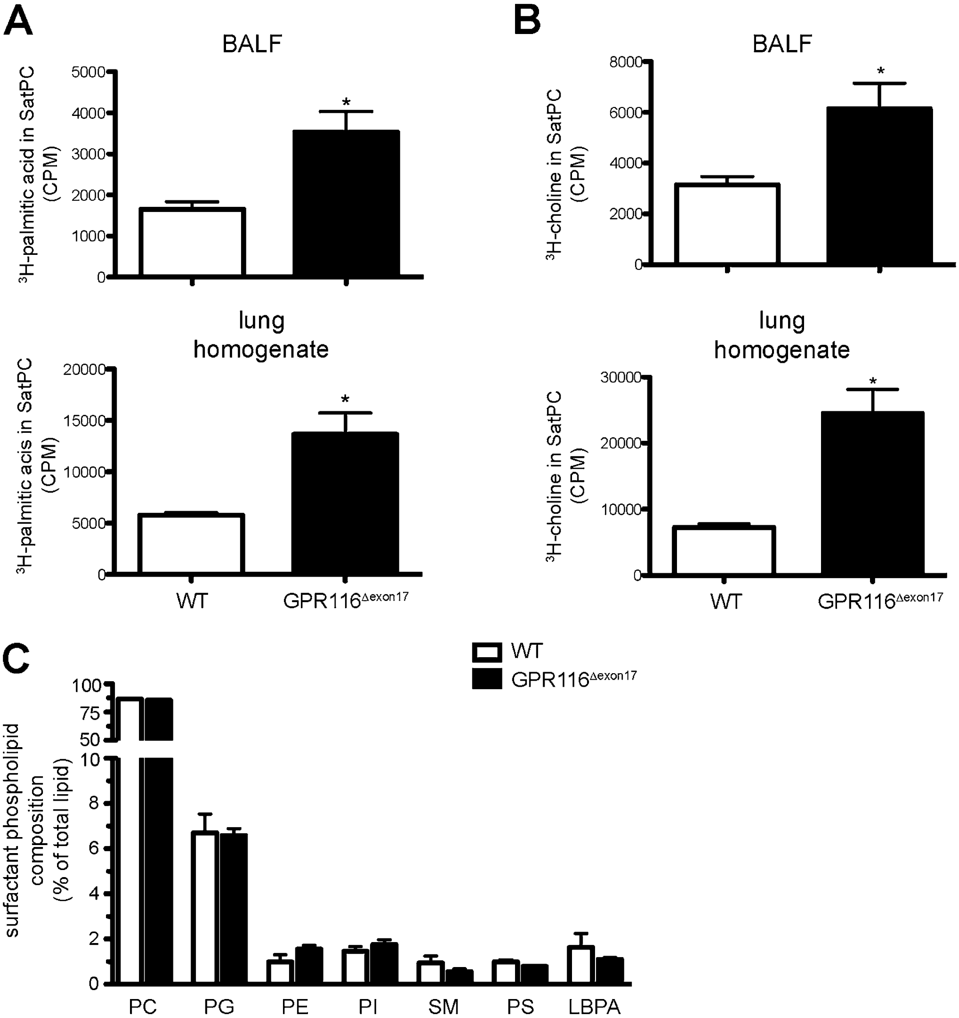

Figure 3. Increased SatPC synthesis and normal surfactant phospholipid composition in *Gpr116$^{\Delta exon17}$* lung tissue. (*A* and *B*) SatPC synthesis, determined by measuring the incorporation of ^{3}H-palmitic acid into SatPC 8 hours after [3H]-palmitic acid injection (*A*) or the incorporation of ^{3}H-choline into SatPC 8 hours after [methyl-3H]-choline chloride injection (*B*), was increased in the BALF and lung homogenate of 4-week-old *Gpr116$^{\Delta exon17}$* mice. *$P < 0.05$ versus WT ($n = 4$–5 mice per genotype). (*C*) The composition of pulmonary surfactant phospholipids in the BALF of *Gpr116$^{\Delta exon17}$* and WT mice are comparable at 4 weeks of age ($n = 4$ mice per genotype). LBPA = lysobisphosphatidic acid; PC = phosphatidylcholine; PE = phosphatidylethanolamine; PG = phosphatidylglycerol; PI = phosphatidylinositol; PS = phosphatidylserine; SM = sphingomyelin.

in these analyses were normalized to recovered BALF volume, and inputs for postlavaged lung homogenates were normalized to total protein. Alveolar levels of surfactant protein A (SFTPA) and SFTPD were unchanged in the BALF from *Gpr116$^{\Delta exon17}$* mice relative to WT mice, whereas mature SFTPB and SFTPC proteins were increased 2.5- and 1.7-fold, respectively (Figures 4A and 4B). In contrast, tissue-associated levels of SFTPB and SFTPC were comparable, whereas SFTPA was decreased 1.8-fold and SFTPD was increased 3.7-fold (Figure 4B). To determine the amount of SFTPB protein that was associated with lamellar bodies (LBs), LBs were isolated from the lung tissue of *Gpr116$^{\Delta exon17}$* and WT mice, and mature SFTPB protein was quantitated. When normalized to total protein content in the isolated LBs, mature SFTPB protein was increased 1.6-fold in *Gpr116$^{\Delta exon17}$* LBs compared with WT LBs (Figure 4C). Taken together, these data demonstrate that the hydrophobic surfactant proteins SFTPB and SFTPC were increased in the BALF of *Gpr116$^{\Delta exon17}$* mice, although not to the same extent as SatPC levels, and that SFTPA and SFTPD levels were selectively altered in the lung tissue of *Gpr116$^{\Delta exon17}$* mice.

Alveolar Enlargement, Inflammation, and Surfactant Ultrastructural Changes in *Gpr116$^{\Delta exon17}$* Mice

Histopathology was performed on lung tissue of 4- and 20-week-old *Gpr116$^{\Delta exon17}$* mice to determine the effects of accumulated surfactant on lung structure. The distal airspaces of *Gpr116$^{\Delta exon17}$* lungs were significantly enlarged at 4 and 20 weeks of age compared with WT control mice (Figures 5A and 5B). The airspace enlargement was associated with the presence of lipid-laden macrophages in 20-week-old *Gpr116$^{\Delta exon17}$* lungs, consistent with the large increase of surfactant phospholipids observed at this age (Figure 5A, *asterisk*; Figure E4B). BAL cell counts and differentials on 4- and 20-week-old animals demonstrated a progressive increase in the total number of macrophages and neutrophils in *Gpr116$^{\Delta exon17}$* lungs (Figure E4C). In addition, a proportion of 20-week-old *Gpr116$^{\Delta exon17}$* animals demonstrated focal clusters of lymphoid cells localized primarily to subpleural regions of the lung (Figure 5B, *arrow*), the majority of which were identified as B220/CD45R+ B cells (Figure E4D). Total protein content, as measured by bicinchoninic acid assay, was increased 2.6-fold in *Gpr116$^{\Delta exon17}$* BALF compared with WT control mice at 4 weeks of age (53.4 ± 1.7 versus 20.9 ± 3.9 μg total protein/body weight, respectively); total protein levels of postlavaged lung homogenate were not statistically different between the two genotypes (data not shown). BALF and lung homogenates from 20-week-old *Gpr116$^{\Delta exon17}$* mice failed to grow bacterial colonies on blood agar plates, indicating the absence of bacterial infection (data not shown). Ultrastructural analysis of secreted surfactant in the alveoli of *Gpr116$^{\Delta exon17}$* mice showed an abundance of aggregated lipid whorls compared with the prototypical "loose" ultrastructure of surfactant seen in the WT lung (Figure 6, *middle panel* versus *left panel*). In addition, *Gpr116$^{\Delta exon17}$* airspaces contained compact, electron-dense surfactant particles that contained tubular myelin structures (Figure 6, *far right panel*).

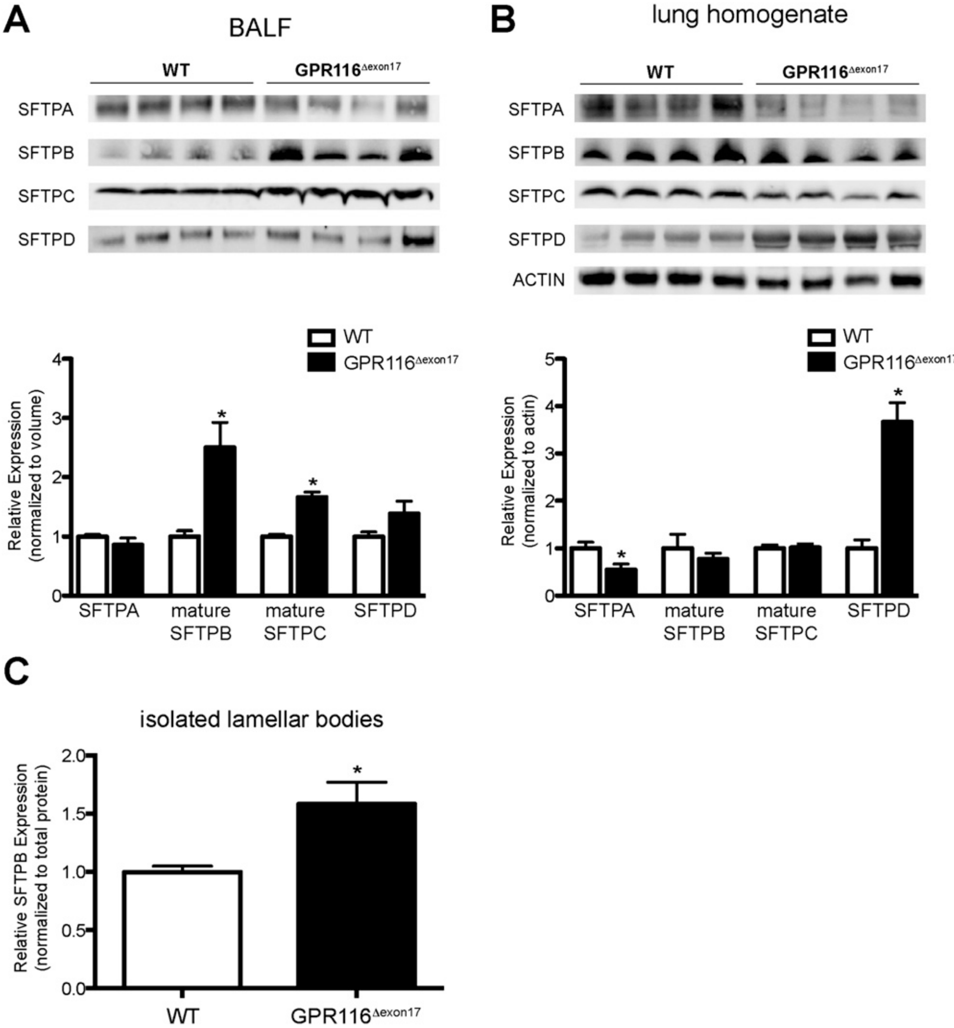

Figure 4. Surfactant protein expression and secretion in GPR116$^{\Delta exon17}$ mice. (*A*) Representative Western blot analyses of surfactant proteins A (SFTPA), B (SFTPB), C (SFTPC), and D (SFTPD) in BALF of *Gpr116*$^{\Delta exon17}$ and WT control mice at 4 weeks of age. Input was normalized to recovered volume of unfractionated BALF; relative molecular weights = 26 to 38 kD (SFTPA), 16 kD (SFTPB), 4 kD (SFTPC), 43 kD (SFTPD), and 44 kD (ACTIN). The *graph* represents n = 7 mice per genotype. (*B*) Representative Western blot analyses of surfactant proteins in postlavaged lung homogenate of *Gpr116*$^{\Delta exon17}$ and WT control mice at 4 weeks of age. Input was normalized to total protein levels, and data were normalized to ACTIN; the *graph* represents n = 4 mice per genotype. (*C*) Quantitation of mature SFTPB protein levels in lamellar bodies isolated from 4-week-old *Gpr116*$^{\Delta exon17}$ and WT mice. Input was normalized to total protein. *$P < 0.05$ versus WT.

Taken together, these data demonstrate an association between surfactant phospholipid accumulation, abnormal ultrastructure of alveolar surfactant, lymphocytic and neutrophilic inflammation, and altered alveolar architecture in *Gpr116*$^{\Delta exon17}$ mice at 20 weeks of age, suggesting that chronic surfactant overload in these animals induces pathophysiological alterations in lung structure and function.

Induction of the Purinergic Receptor P2RY2 in *Gpr116*$^{\Delta exon17}$ Mice

Due to the marked accumulation of surfactant in *Gpr116*$^{\Delta exon17}$ mice associated with increased SatPC synthesis, we hypothesized that GPR116 primarily regulates surfactant phospholipid synthesis genes at the transcriptional level. To test this hypothesis using an unbiased approach, we compared the transcriptomes of purified type II cells from 4-week-old *Gpr116*$^{\Delta exon17}$ and WT control mice by RNA microarray analysis (n = 3 mice per genotype). Data from this experiment has been submitted to Gene Expression Omnibus (accession number GSE41417). Very few transcriptional changes were detected in *Gpr116*$^{\Delta exon17}$ type II cells, including differences in genes required for surfactant phospholipid synthesis (Figure E5). In fact, several phospholipid synthesis genes were significantly decreased in *Gpr116*$^{\Delta exon17}$ type II cells, including *Acox2*, *Chpt1*, and *Slc2a1* (Figure E4). Levels of *Il-4* and *Csf2* (also known as *Gmcsf*), genes that are known to alter surfactant homeostasis (26, 31), were comparable in *Gpr116*$^{\Delta exon17}$ and control mice, as were mRNA levels of all of the surfactant proteins (Figure E5 and data not shown). However, while analyzing the data for genes related to surfactant secretion, we found that the purinergic receptor, P2RY2, was increased 2.1-fold in *Gpr116*$^{\Delta exon17}$ type II cells. Induction of P2RY2 mRNA was confirmed by qPCR in purified type II cells and in the lung homogenate of *Gpr116*$^{\Delta exon17}$ mice (Figures 7A and 7B). P2RY2 was significantly increased in *Gpr116*$^{\Delta exon17}$ lung tissue at E18.5, a time point at which SatPC levels were normal (Figure 2A). Increased P2RY2 mRNA expression correlated with a 1.9-fold increase in P2RY2 protein in whole lung homogenate of 4-week-old *Gpr116*$^{\Delta exon17}$ mice (Figures 7C and 7D).

DISCUSSION

The goal of this study was to define the role of GPR116 in pulmonary surfactant homeostasis. Our data show that expression of GPR116 in the murine lung was developmentally regulated, reaching maximal levels 1 day after birth, with sustained expression through adulthood. We further demonstrated that GPR116 protein was highly expressed on the apical membrane of alveolar type I and type II epithelial cells and on cilia of proximal epithelia but is not expressed on alveolar macrophages or pulmonary endothelial cells. GPR116 loss-of-function mice developed marked increases in alveolar surfactant phospholipids and proteins that began postnatally and progressed with age. Increased

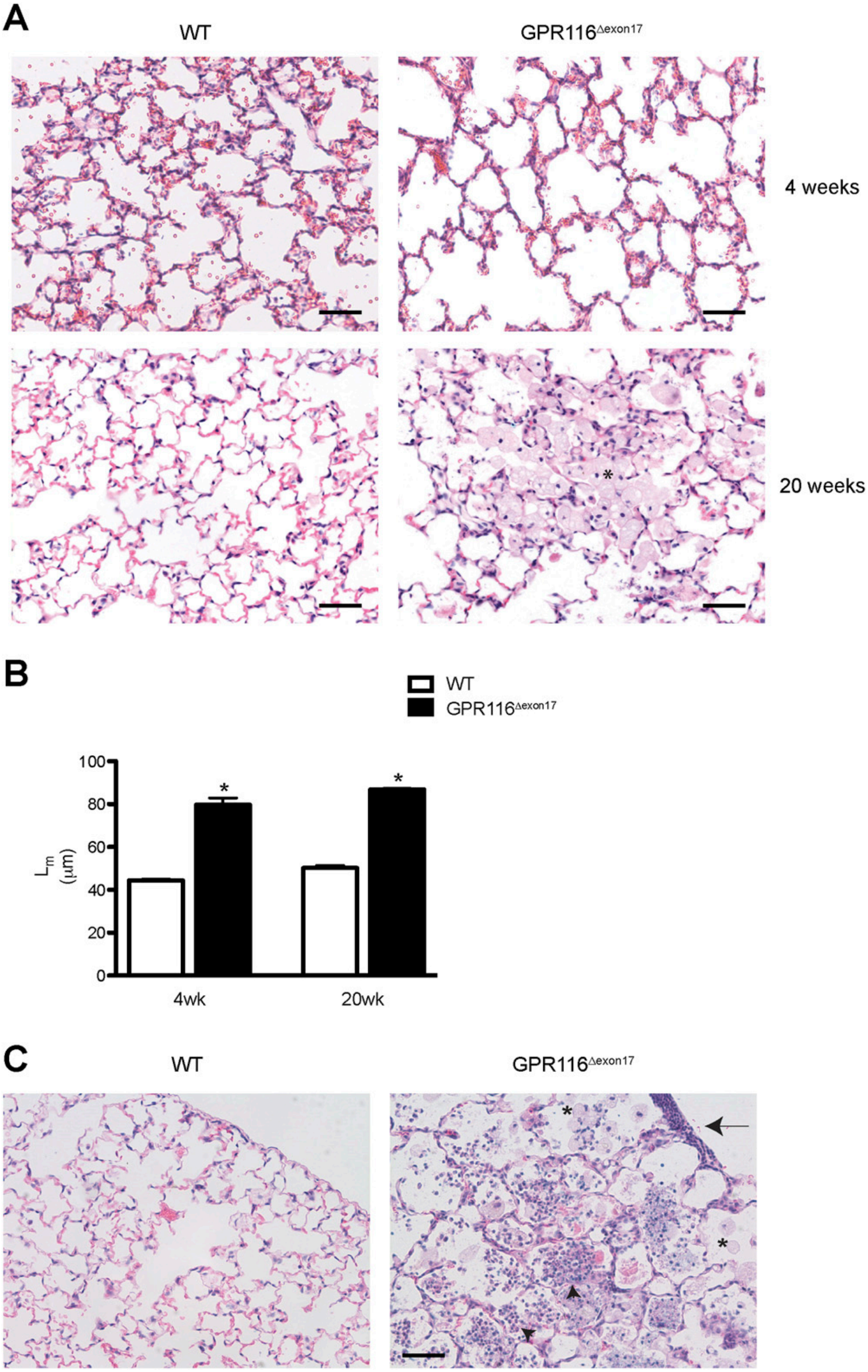

Figure 5. Alveolar simplification and inflammation in *Gpr116*$^{\Delta exon17}$ mice. (*A*) Representative hematoxylin and eosin–stained lung sections from 4- and 20-week-old animals. Note enlarged alveoli at 4 and 20 weeks and the presence of lipid-laden macrophages (*asterisk*) in *Gpr116*$^{\Delta exon17}$ lungs at 20 weeks of age. (*B*) Mean linear intercept quantitation demonstrates enlarged airspaces in *Gpr116*$^{\Delta exon17}$ mice at 4 weeks (1.8-fold) and 20 weeks (1.7-fold) ($n = 3$ mice per genotype). *$P < 0.05$ versus WT. (*C*) Subpleural accumulation of lymphoid cells (*arrow*), neutrophilia (*arrowheads*), and foamy alveolar macrophages (*asterisks*) in 20-week-old *Gpr116*$^{\Delta exon17}$ animals. *Scale bars* = 50 μm.

surfactant in *Gpr116*$^{\Delta exon17}$ animals was associated with augmented SatPC synthesis and an increased SatPC alveolar-tissue index in juvenile animals, the presence of inflammatory infiltrates (including lipid-laden macrophages), and alveolar enlargement. Microarray analyses demonstrated that surfactant phospholipid synthesis genes were not induced in purified *Gpr116*$^{\Delta exon17}$ type II cells, suggesting that the principle mechanism by which GPR116 regulates surfactant pool size is not at the level of transcription of surfactant synthesis genes. However, we found that P2RY2, a GPCR known to mediate surfactant secretion (5, 6), was significantly increased at the mRNA and protein level in 4-week-old *Gpr116*$^{\Delta exon17}$ type II cells associated with increased SatPC levels in the media of cultured primary *Gpr116*$^{\Delta exon17}$ type II cells. Collectively, these data demonstrate that GPR116 is a major regulator of surfactant homeostasis and are consistent with the hypothesis that GPR116 maintains alveolar surfactant pool sizes via control of the regulated secretory pathway in alveolar type II cells.

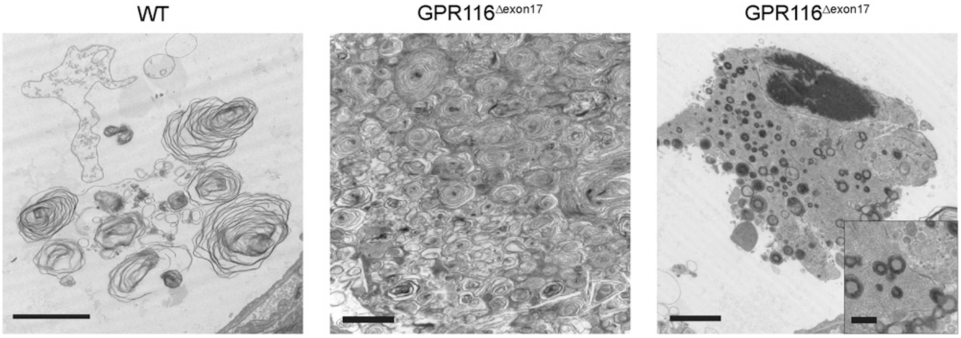

Figure 6. Ultrastructural analysis of secreted surfactant in *Gpr116*$^{\Delta exon17}$ mice. (*A*) Representative electron micrographs of WT and *Gpr116*$^{\Delta exon17}$ lung sections at 20 weeks showing morphology of secreted surfactant within an alveolus. Note the abundance and dense, aggregated nature of surfactant in the *Gpr116*$^{\Delta exon17}$ lung compared with prototypical ultrastructure seen in the WT lung. *Scale bar* in *large panels* = 2 mm; *scale bar* in *inset* = 500 nm.

The targeting strategy used to engineer the *Gpr116*$^{f/f}$ allele was intended to fully ablate the function of GPR116 by eliminating all seven transmembrane domains of the protein upon Cre-mediated excision. Through initial characterization, we demonstrated that the *Gpr116*$^{\Delta exon17}$ allele produces a protein that is low in abundance and mislocalized compared with WT GPR116 (Figure E3). Based on these data, the increased surfactant pool sizes in *Gpr116*$^{\Delta exon17}$ mice could be due to loss-of-function of the WT protein or to gain-of-function of the GPR116$^{\Delta exon17}$ protein. Two key pieces of data argue against a gain-of-function explanation for the observed phenotype. First, mice heterozygous for the *Gpr116*$^{\Delta exon17}$ allele were healthy and fertile, had SatPC levels comparable to WT mice at 6 months of age, and lacked histological pulmonary abnormalities (data not shown). Second, the surfactant accumulation phenotype in *Gpr116*$^{\Delta exon17}$ mice was identical to that reported (in abstract form) for a distinct GPR116 loss-of-function mouse in which exon1 was replaced with a *lacZ* reporter (32). These data strongly support the concept that the surfactant accumulation in *Gpr116*$^{\Delta exon17}$ mice was due to a loss-of-function and demonstrate that the transmembrane domains of GPR116 are critically required for its function *in vivo*.

Similar to *Gpr116*$^{\Delta exon17}$ mice, increased alveolar surfactant pool sizes were observed in *Sftpd*$^{-/-}$ and *Csf2*$^{-/-}$ mice (33–35). In addition, mutations in the α chain of the *CSF2* receptor, *CSF2R* (36, 37), or autoantibodies against CSF2 itself (38) cause primary pulmonary alveolar lipoproteinosis in humans. Detailed analyses of surfactant metabolism *in vivo* in *Sftpd*$^{-/-}$ and *Csf2*$^{-/-}$ mice have shown that neither surfactant synthesis nor secretion was increased in these models (13, 26, 39). Rather, the defect was attributed to defective uptake and/or catabolism of surfactant by type II cells and alveolar macrophages due to altered surfactant ultrastructure (*Sftpd*$^{-/-}$ [40]) or impaired macrophage differentiation (*Csf2*$^{-/-}$ [41]). In contrast, SatPC synthesis and the SatPC alveolar-tissue SatPC index were significantly increased in 4-week-old *Gpr116*$^{\Delta exon17}$ mice. These increases occurred before the abundant accumulation of lipid-laden macrophages observed in older animals, suggesting that the primary defect is due to surfactant hypersecretion rather than to defective surfactant catabolism. Furthermore, *Gpr116* is not detectable on alveolar macrophages, and P2RY2, a receptor known to stimulate surfactant secretion in an ATP/UTP-dependent manner (6, 10), was increased in *Gpr116*$^{\Delta exon17}$ type II cells associated with increased SatPC levels in the media of cultured *Gpr116*$^{\Delta exon17}$ type II cells. Mouse models of the human disease Hermansky-Pudlak syndrome also demonstrate altered surfactant homeostasis. However, unlike *Gpr116*$^{\Delta exon17}$, *Sftpd*$^{-/-}$, and *Csf2*$^{-/-}$ mice, mice with mutations in Hermansky-Pudlak syndrome–associated genes exhibit decreased alveolar pools of surfactant phospholipids and increased tissue phospholipid levels due to defects in surfactant trafficking and decreased secretion in type II cells (42–44). Taken together, our data support the hypothesis that GPR116 controls alveolar surfactant pool sizes by negatively regulating surfactant secretion from type II cells.

Although GPR116 expression is highest in the lung, GPR116 mRNA is detected in multiple organs, including adipose tissue (Figure 1A). Recent data reported by Nie and colleagues implicate a role for GPR116 in adipocyte differentiation and energy homeostasis. In this study, knockdown of GPR116 in 3T3-L1 cells resulted in impaired differentiation into adipocytes

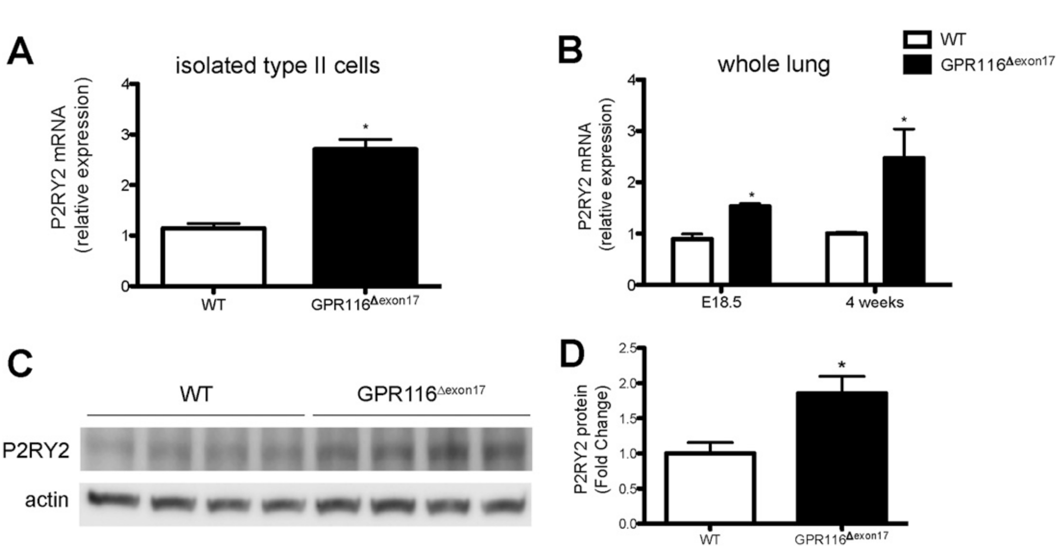

Figure 7. The purinergic receptor P2RY2 is increased in *Gpr116*$^{\Delta exon17}$ lungs. (*A* and *B*) qPCR analysis demonstrating increased expression of P2RY2 in type II cells isolated from *GPR116*$^{\Delta exon17}$ mice at 4 weeks of age (*A*) and in whole lung tissue at E18.5 and 4 weeks of age (*B*). **P* < 0.05 versus WT at respective time points (*n* = 4 lungs per group). (*C*) P2RY2 protein expression by Western blot analysis of whole lung homogenates from 4-week-old animals. (*D*) Densitometry analysis of the data in *C* demonstrates a 1.9-fold increase in *Gpr116*$^{\Delta exon17}$ lungs. **P* < 0.05 versus WT.

in vitro, and adipocyte-specific ablation of GPR116 function *in vivo* resulted in increased susceptibility to high-fat diet–induced glucose intolerance and insulin resistance (45). It is unknown if GPR116 ablation in adipocytes or other GPR116-expressing tissues contributed to altered surfactant homeostasis in *Gpr116*$^{\Delta exon17}$ mice.

The endogenous ligand and intracellular pathways by which GPR116 signals to control surfactant homeostasis are unknown. Expression of GPR116 on the apical surface of type I and type II epithelial cells (Figure 1D and Ref. 28) suggests that the ligand resides in the alveolar subphase fluid and/or is a component of pulmonary surfactant. Our microarray analysis demonstrated that P2RY2 expression is increased in the absence of GPR116 function. Therefore, one possible mechanism by which GPR116 functions is by regulating P2RY2 expression to control surfactant secretion. Alternatively, because GPCRs of the melatonin receptor subfamily (46) and human cytomegalovirus encoded GPCRs (47) are known to functionally inhibit each other via heterodimerization, GPR116 may also negatively control P2RY2 activity or the activity of other GPCRs involved in surfactant secretion, including β_2AR or A_{2B}, via heterodimerization to effect secretion. *P2ry2*$^{-/-}$ mice do not display an overt pulmonary phenotype in the absence of challenge, indicating that P2RY2 is dispensable for baseline pulmonary function (48). However, these data do not preclude the possibility that increased P2RY2 expression and/or activity is driving surfactant accumulation in *Gpr116*$^{\Delta exon17}$ mice. It is also possible that GPR116 controls surfactant homeostasis independent of surfactant secretion by positively regulating surfactant uptake and catabolism after ligand engagement directly within type II cells or indirectly through alveolar macrophages.

It is unclear whether type I– or type II–specific expression of GPR116, or expression on both cell types, is required for surfactant homeostasis. Experimental evidence supports a role for type I/type II cell crosstalk in regulating surfactant secretion. Calcium imaging studies in an isolated rat lung model demonstrated that alveolar expansion rapidly increased intracellular calcium levels in type I and type II cells, triggering surfactant secretion (49). Inhalation-induced surfactant exocytosis in this model was inhibited by intracellular calcium chelation and by functional blockade of intracellular gap junctions, demonstrating a role for type I/type II cell communication in regulated secretion. Furthermore, mechanical stretch of cocultured rat "type I–like" cells (transdifferentiated from type II cells in culture) and type II cells resulted in type I–mediated ATP release that stimulated surfactant secretion from type II cells (50). Recent data using similar coculture techniques demonstrated that activation of a type I–specific purinergic receptor, P2RX7, was sufficient to release ATP from type I cells, triggering P2RY2-dependent surfactant release from type II cells (51).

Collectively, our data support a working model in which GPR116 is highly induced during the later stages of lung development and is poised for activation in the perinatal lung. After the burst of surfactant secretion from type II cells that promotes the transition to air breathing at birth, a newly presented ligand in the alveolar space binds to the extracellular domain of GPR116 on alveolar epithelial cells, activating downstream signaling pathways to regulate surfactant secretion via suppression of P2RY2 expression and/or activity or to regulate surfactant uptake and degradation by type II cells and/or macrophages to maintain alveolar surfactant pool sizes at homeostatic levels. The long-term goal of this work is to identify potential therapeutic targets, including GPR116 itself, for modulating endogenous surfactant levels in the treatment of lung diseases associated with surfactant dysfunction.

Author disclosures are available with the text of this article at www.atsjournals.org.

Acknowledgments: The authors thank Shawn Grant, Angelica Schehr, Angie Keiser, Emily Reno, Catherine Cannet, Thomas Suply, and Juan Zhang for excellent technical assistance and Klaus Seuwen for insightful discussions.

References

1. Hawgood S, Clements JA. Pulmonary surfactant and its apoproteins. *J Clin Invest* 1990;86:1–6.
2. Veldhuizen R, Nag K, Orgeig S, Possmayer F. The role of lipids in pulmonary surfactant. *Biochim Biophys Acta* 1998;1408:90–108.
3. Notter RH. Lung surfactants: basic science and clinical applications. New York: Marcel Dekker; 2000.
4. Goerke J. Pulmonary surfactant: functions and molecular composition. *Biochim Biophys Acta* 1998;1408:79–89.
5. Rice WR, Singleton FM. P2-purinoceptors regulate surfactant secretion from rat isolated alveolar type II cells. *Br J Pharmacol* 1986;89:485–491.
6. Gilfillan AM, Rooney SA. Purinoceptor agonists stimulate phosphatidylcholine secretion in primary cultures of adult rat type II pneumocytes. *Biochim Biophys Acta* 1987;917:18–23.
7. Dobbs LG, Mason RJ. Pulmonary alveolar type II cells isolated from rats: release of phosphatidylcholine in response to beta-adrenergic stimulation. *J Clin Invest* 1979;63:378–387.
8. Mettler NR, Gray ME, Schuffman S, LeQuire VS. Beta-adrenergic induced synthesis and secretion of phosphatidylcholine by isolated pulmonary alveolar type II cells. *Lab Invest* 1981;45:575–586.
9. Brown LA, Longmore WJ. Adrenergic and cholinergic regulation of lung surfactant secretion in the isolated perfused rat lung and in the alveolar type II cell in culture. *J Biol Chem* 1981;256:66–72.
10. Gilfillan AM, Rooney SA. Functional evidence for adenosine A2 receptor regulation of phosphatidylcholine secretion in cultured type II pneumocytes. *J Pharmacol Exp Ther* 1987;241:907–914.
11. Griese M, Gobran LI, Douglas JS, Rooney SA. Adenosine A2-receptor-mediated phosphatidylcholine secretion in type II pneumocytes. *Am J Physiol* 1991;260:L52–L60.
12. Wirtz HR, Dobbs LG. Calcium mobilization and exocytosis after one mechanical stretch of lung epithelial cells. *Science* 1990;250:1266–1269.
13. Ikegami M, Whitsett JA, Jobe A, Ross G, Fisher J, Korfhagen T. Surfactant metabolism in SP-D gene-targeted mice. *Am J Physiol Lung Cell Mol Physiol* 2000;279:L468–L476.
14. Rebello CM, Jobe AH, Eisele JW, Ikegami M. Alveolar and tissue surfactant pool sizes in humans. *Am J Respir Crit Care Med* 1996; 154:625–628.
15. Jobe A, Ikegami M, Jacobs H. Changes in the amount of lung and airway phosphatidylcholine in 0.5–12.5-day-old rabbits. *Biochim Biophys Acta* 1981;664:182–187.
16. Ikegami M. Surfactant catabolism. *Respirology* 2006;11:S24–S27.
17. Rice WR, Hull WM, Dion CA, Hollinger BA, Whitsett JA. Activation of cAMP dependent protein kinase during surfactant release from type II pneumocytes. *Exp Lung Res* 1985;9:135–149.
18. Sano K, Voelker DR, Mason RJ. Involvement of protein kinase C in pulmonary surfactant secretion from alveolar type II cells. *J Biol Chem* 1985;260:12725–12729.
19. Voyno-Yasenetskaya TA, Dobbs LG, Williams MC. Regulation of ATP-dependent surfactant secretion and activation of second-messenger systems in alveolar type II cells. *Am J Physiol* 1991;261:105–109.
20. Liu L. Inhibition of lung surfactant secretion by KN-62, a specific inhibitor of the calcium- and calmodulin-dependent protein kinase II. *Biochem Mol Biol Int* 1998;45:823–830.
21. Mason RJ, Williams MC, Greenleaf RD, Clements JA. Isolation and properties of type II alveolar cells from rat lung. *Am Rev Respir Dis* 1977;115:1015–1026.
22. Nicholas TE, Barr HA. The release of surfactant in rat lung by brief periods of hyperventilation. *Respir Physiol* 1983;52:69–83.
23. Bligh EG, Dyer WJ. A rapid method of total lipid extraction and purification. *Can J Biochem Physiol* 1959;37:911–917.
24. Mason RJ, Nellenbogen J, Clements JA. Isolation of disaturated phosphatidylcholine with osmium tetroxide. *J Lipid Res* 1976;17: 281–284.

25. Ikegami M, Dhami R, Schuchman EH. Alveolar lipoproteinosis in an acid sphingomyelinase-deficient mouse model of Niemann-Pick disease. *Am J Physiol Lung Cell Mol Physiol* 2003;284:L518–L525.
26. Ikegami M, Ueda T, Hull W, Whitsett JA, Mulligan RC, Dranoff G, Jobe AH. Surfactant metabolism in transgenic mice after granulocyte macrophage-colony stimulating factor ablation. *Am J Physiol* 1996;270:L650–L658.
27. Bridges JP, Ikegami M, Brilli LL, Chen X, Mason RJ, Shannon JM. LPCAT1 regulates surfactant phospholipid synthesis and is required for transitioning to air breathing in mice. *J Clin Invest* 2010;120:1736–1748.
28. Abe J, Suzuki H, Notoya M, Yamamoto T, Hirose S. Ig-hepta, a novel member of the G protein-coupled hepta-helical receptor (GPCR) family that has immunoglobulin-like repeats in a long N-terminal extracellular domain and defines a new subfamily of GPCRs. *J Biol Chem* 1999;274:19957–19964.
29. Wallgard E, Larsson E, He L, Hellström M, Armulik A, Nisancioglu MH, Genove G, Lindahl P, Betsholtz C. Identification of a core set of 58 gene transcripts with broad and specific expression in the microvasculature. *Arterioscler Thromb Vasc Biol* 2008;28:1469–1476.
30. Daneman R, Zhou L, Agalliu D, Cahoy JD, Kaushal A, Barres BA. The mouse blood-brain barrier transcriptome: a new resource for understanding the development and function of brain endothelial cells. *PLoS ONE* 2010;5:e13741.
31. Ikegami M, Whitsett JA, Chroneos ZC, Ross GF, Reed JA, Bachurski CJ, Jobe AH. IL-4 increases surfactant and regulates metabolism in vivo. *Am J Physiol Lung Cell Mol Physiol* 2000;278:L75–L80.
32. Ichinose T, Fukuzawa T, Kato A, Ikegami M, Ishida J, Hirose S. Pulmonary surfactant accumulation in Ig-Hepta/GPR116 knockout mice. *J Physiol Sci* 2009;59:269.
33. Korfhagen TR, Sheftelyevich V, Burhans MS, Bruno MD, Ross GF, Wert SE, Stahlman MT, Jobe AH, Ikegami M, Whitsett JA, *et al.* Surfactant protein-D regulates surfactant phospholipid homeostasis in vivo. *J Biol Chem* 1998;273:28438–28443.
34. Botas C, Poulain F, Akiyama J, Brown C, Allen L, Goerke J, Clements J, Carlson E, Gillespie AM, Epstein C, *et al.* Altered surfactant homeostasis and alveolar type II cell morphology in mice lacking surfactant protein D. *Proc Natl Acad Sci USA* 1998;95:11869–11874.
35. Dranoff G, Crawford AD, Sadelain M, Ream B, Rashid A, Bronson RT, Dickersin GR, Bachurski CJ, Mark EL, Whitsett JA, *et al.* Involvement of granulocyte-macrophage colony-stimulating factor in pulmonary homeostasis. *Science* 1994;264:713–716.
36. Suzuki T, Sakagami T, Rubin BK, Nogee LM, Wood RE, Zimmerman SL, Smolarek T, Dishop MK, Wert SE, Whitsett JA, *et al.* Familial pulmonary alveolar proteinosis caused by mutations in CSF2RA. *J Exp Med* 2008;205:2703–2710.
37. Martinez-Moczygemba M, Doan ML, Elidemir O, Fan LL, Cheung SW, Lei JT, Moore JP, Tavana G, Lewis LR, Zhu Y, *et al.* Pulmonary alveolar proteinosis caused by deletion of the GM-CSFRalpha gene in the X chromosome pseudoautosomal region 1. *J Exp Med* 2008;205: 2711–2716.
38. Kitamura T, Tanaka N, Watanabe J, Uchida, Kanegasaki S, Yamada Y, Nakata K. Idiopathic pulmonary alveolar proteinosis as an autoimmune disease with neutralizing antibody against granulocyte/macrophage colony-stimulating factor. *J Exp Med* 1999;190:875–880.
39. Ellgaard L, Helenius A. ER quality control: towards an understanding at the molecular level. *Curr Opin Cell Biol* 2001;13:431–437.
40. Ikegami M, Na CL, Korfhagen TR, Whitsett JA. Surfactant protein D influences surfactant ultrastructure and uptake by alveolar type II cells. *Am J Physiol Lung Cell Mol Physiol* 2005;288:L552–L561.
41. Shibata Y, Berclaz PY, Chroneos ZC, Yoshida M, Whitsett JA, Trapnell BC. GM-CSF regulates alveolar macrophage differentiation and innate immunity in the lung through PU.1. *Immunity* 2001;15:557–567.
42. Atochina-Vasserman EN, Bates SR, Zhang P, Abramova H, Zhang Z, Gonzales L, Tao JQ, Gochuico BR, Gahl W, Guo CJ, *et al.* Early alveolar epithelial dysfunction promotes lung inflammation in a mouse model of Hermansky-Pudlak syndrome. *Am J Respir Crit Care Med* 2011;184:449–458.
43. Guttentag SH, Akhtar A, Tao JQ, Atochina E, Rusiniak ME, Swank RT, Bates SR. Defective surfactant secretion in a mouse model of Hermansky-Pudlak syndrome. *Am J Respir Cell Mol Biol* 2005;33:14–21.
44. Lyerla TA, Rusiniak ME, Borchers M, Jahreis G, Tan J, Ohtake P, Novak EK, Swank RT. Aberrant lung structure, composition, and function in a murine model of Hermansky-Pudlak syndrome. *Am J Physiol Lung Cell Mol Physiol* 2003;285:L643–L653.
45. Nie T, Hui X, Gao X, Li K, Lin W, Xiang X, Ding M, Kuang Y, Xu A, Fei J, *et al.* Adipose tissue deletion of Gpr116 impairs insulin sensitivity through modulation of adipose function. *FEBS Lett* 2012; 586:3618–3625.
46. Levoye A, Dam J, Ayoub MA, Guillaume JL, Couturier C, Delagrange P, Jockers R. The orphan GPR50 receptor specifically inhibits MT1 melatonin receptor function through heterodimerization. *EMBO J* 2006;25:3012–3023.
47. Tschische P, Tadagaki K, Kamal M, Jockers R, Waldhoer M. Heteromerization of human cytomegalovirus encoded chemokine receptors. *Biochem Pharmacol* 2011;82:610–619.
48. Homolya L, Watt WC, Lazarowski ER, Koller BH, Boucher RC. Nucleotide-regulated calcium signaling in lung fibroblasts and epithelial cells from normal and P2Y(2) receptor (−/−) mice. *J Biol Chem* 1999;274:26454–26460.
49. Ashino Y, Ying X, Dobbs LG, Bhattacharya J. [Ca(2+)](i) oscillations regulate type II cell exocytosis in the pulmonary alveolus. *Am J Physiol Lung Cell Mol Physiol* 2000;279:L5–L13.
50. Patel AS, Reigada D, Mitchell CH, Bates SR, Margulies SS, Koval M. Paracrine stimulation of surfactant secretion by extracellular ATP in response to mechanical deformation. *Am J Physiol Lung Cell Mol Physiol* 2005;289:L489–L496.
51. Mishra A, Chintagari NR, Guo Y, Weng T, Su L, Liu L. Purinergic P2X7 receptor regulates lung surfactant secretion in a paracrine manner. *J Cell Sci* 2011;124:657–668.